Chem Soc Rev

Poly(aryleneethynylene)s (PAE) as paradigmatic sensor cores

Journal:	*Chemical Society Reviews*
Manuscript ID:	CS-REV-08-2014-000267.R1
Article Type:	Review Article
Date Submitted by the Author:	28-Aug-2014
Complete List of Authors:	Bunz, Uwe; Ruprecht-Karls Universität Heidelberg, Organisch-Chemisches Institut Bender, Markus; Ruprecht-Karls Universität Heidelberg, Organisch-Chemisches Institut Seehafer, Kai; Ruprecht-Karls Universität Heidelberg, Organisch-Chemisches Institut Porz, Michael; Organisch-Chemisches Institut,

SCHOLARONE™
Manuscripts

Chem. Soc. Rev

REVIEW ARTICLE

# Poly(aryleneethynylene)s (PAE) as paradigmatic sensor cores

Uwe H. F. Bunz,*[a,b] Kai Seehafer,[a] Markus Bender,[a] and Michael Porz[a]

We describe poly(aryleneethynylene)s (PAE) as powerful sensor cores. We discuss concepts (super quenching, molecular wire effect, multivalency) that were developed using PAEs and also the relationship that connect side chain structure (polar, polyelectrolyte, *etc.*, number of ionic groups per repeat, position) and optical properties such as quantum yields. In the second part of the review we discuss applications of PAEs in their interaction with sensor targets; metal cations, fluoride and other anions, explosives, proteins and whole cells beeing the target for PAEs, while cationic PAEs have been used for the transfection of eukaryotic cells with RNA.

Uwe Bunz (born 1963 in Neheim-Hüsten) obtained his Dr. rer. nat. 1990, was promoted to Associate Professor in 1997 and Full Professor (U of South Carolina) in 2001. In 2003 he moved to the Georgia Institute of Technology and since 2010 he is Chaired Professor (Lehrstuhl I) at the Organisch-Chemisches Institut in Heidelberg. His research interests are conjugated semiconducting materials and alkyne chemistry. He has published over 250 papers. His hobbies are swimming, surfing, cooking, baking and MMORPGs.
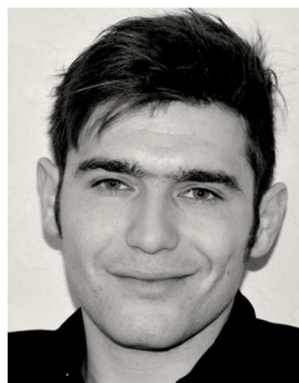
Markus Bender (born 1987 in Schwäbisch Hall) obtained his M. Sc. 2013 in the Bunz group working on the synthesis of novel water soluble polymers of the poly(aryleneethynylene) type. He works closely with Dr. Seehafer. Since January 2014 he pursues his PhD thesis in the Bunz group, exploring novel macromolecular architectures applicable for sensing and organic electronics. His hobbies are weight lifting, motorcycle riding and traveling.

Kai Seehafer (born 1983 in Neustadt an der Weinstraße) obtained his Dipl. Chem. with Prof. C. Koch-Brandt (Uni Mainz, 2009) characterizing a receptor-mediated cell pathway. He then obtained his PhD with Prof. G. Helmchen (Uni Heidelberg, 2012) working on the synthesis of natural products. Since March 2013 he is working as a senior research associate in the Bunz group. His research interests are water soluble conjugated polymers of the poly(aryleneethynylene) type. His hobbies are running, traveling and cooking.

Michael Porz (born 1984 in Karlsruhe) obtained his diploma in chemistry 2011 in the Bunz group working on alkene metathesis and ROMP of novel conjugated monomers. Since August 2011, he has been working on his PhD thesis in the Bunz group, exploring novel macromolecular architectures applicable for organic electronics. His hobbies are volleyball, surfing and cycling.

TOC
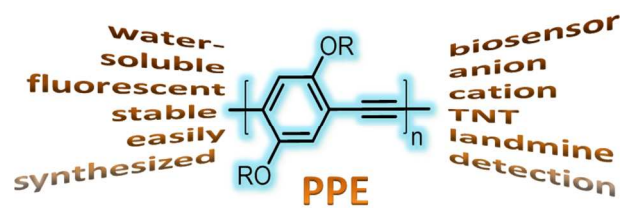
What you need to know about poly(aryleneethynylene)s as sensory materials. A tutorial of fundamental properties and new developments since 2009.

1 Introduction and scope

The term sensor target is ambigous. Sensor targets can be both, sensory materials employed and analytes investigated. In this contribution we discuss polymeric sensors that are composed of arene groups separated by alkyne units. The poly(aryleneethynylene)s (PAE) are conjugated, *i.e.* semiconducting, polymers that show absorbance and fluorescence in the visible spectrum. Many (but not all) PAEs are linear; their optical properties depend upon the twist angle of neighbouring aryl groups, with coplanar conformers showing lower band gaps and red-shifted absorption and emission through enhanced conjugation. [1,2]

The simplest PAEs are the poly(*para*-phenyleneethynylene)s (PPE) **1**.[3] The representatives that are useful for sensing applications carry alkoxy-type side chains, as the starting materials for such PPEs are easily obtained by base-promoted functionalization of 1,4-diiodo-2,5-hydroquinone and subsequent alkynylation through a Sonogashira coupling into *para*-diethynylated dialkoxy-benzenes. The Pd-catalyzed coupling of aromatic diiodides to aromatic diynes then gives the PPE (and other PAEs) in good yields and with degrees of polymerization (P_n) that range from 20 to around 200. In certain cases, a higher P_n can be reached.[4] The combination of alkoxybenzenes in the Pd-catalyzed synthesis of PAEs introduces almost any functional group. The alkylation of phenols and the Pd-catalyzed coupling of the Sonogashira-type[5] work under mild conditions. The lateral attachment of esters, sugars, branched, linear and functionalized oligoethyleneglycols *etc.* are feasible. This approach favours polymers with two sets of different side groups, as an alternating AB-type polymer structure is the naturally obtained one for this synthesis of PAEs. One can use two different arene building blocks, increasing the variability and achievable structural and property space to construct responsive polymers for almost any purpose.

1
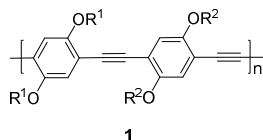
A fundamental property of PPEs, and in many cases also of PAEs, is their high emissive quantum yield in organic solvents and in thin films; some PAEs show high emissive quantum yields in water when carrying suitable substituents (see Figure 1).

1.1 Scope and limitations

There are multitudes of sensors and dosimeters based on conjugated polymers. We restrict ourselves to sensors and dosimeters based upon PAEs. PAEs are easily synthesized and often show exquisitely sensitive changes of fluorescence when exposed to analytes. These properties justify the choice of PAEs as sensors. We will use the term "sensor" loosely, also for dosimeters. A sensor binds reversibly to an analyte and detects the presence of the analyte through the change of a property that can be observed. A dosimeter is similar, but the

binding is irreversible, *i.e.* even when the analyte is removed, the response does not disappear.

Canonical cases, where basic principles were established are discussed, followed by selected newer developments that have appeared after 2009, when the field of PAEs was last comprehensively reviewed.[3] The scope of this review includes structures, synthetic details where important; optical properties, sensing mechanisms and sensing applications of PAEs.

1.2 Synthesis of PAEs

Several reviews deal with the syntheses and properties of PAEs, dispensing synthetic advice as how to prepare PAEs (Table 1). We recommend coupling of aryl diiodides with aromatic diynes using $(Ph_3P)_2PdCl_2$ as catalyst with low (0.1-0.2 mol%) loadings and piperidine/THF as solvent/base mixture at reaction temperatures of 20-80 °C. Higher temperatures can give PAEs of higher molecular weight. If the monomers are sensitive towards piperidine, triethylamine is a suitable surrogate. For aryl bromides, piperidine is not ideal, but triethylamine in the presence of THF is preferred.[6] Generally, high reaction temperatures (> 80 °C) are necessary, unless the bromides are attached to electron poor arenes, which increase reactivity towards the Sonogashira reaction.

Table 1. Some reviews in the field of PAEs and conjugated polymer sensors

First author	Journal	Citation
L. Feng	*Chem. Soc. Rev.*	2013, **42**, 6620
U. H. F. Bunz	*Practical Polymer Synthesis, Ed. Müllen et. al.*	2013, 156-179
C. Zhu	*Chem. Rev.*	2012, **112**, 4687
A. Alvarez	*Trends Anal. Chem.*	2011, **30**, 1513
U. H. F. Bunz	*Angew. Chem. Int. Ed.*	2010, **49**, 3268
F. Feng	*Macromol. Rapid Commun.*	2010, **31**, 1405
Y. Liu	*J. Photochem. Photobiol. C*	2009, **10**, 173
U. H. F. Bunz	*Macromol. Rapid Commun.*	2009, **30**, 772
D. A. M. Egbe	*Prog. Polym. Sci.*	2009, **34**, 1023
J. Liu	*Chem. Rev.*	2009, **109**, 5799
S. W. Thomas	*Chem. Rev.*	2007, **107**, 1339
T. Aoki	*Polymer*	2006, **47**, 4867
C. Weder	*Chem. Commun.*	2005, 5378
C. Weder, Editor	*Adv. Polym. Sci.*	2005, Vol. **177**
F. Babudri	*J. Mater. Chem.*	2004, **14**, 11
T. Yamamoto	*Synlett*	2003, 425
U. H. F. Bunz	*Acc. Chem. Res.*	2001, **34**, 998
T. D. McQuade	*Chem. Rev*	2000, **100**, 2537
U. H. F. Bunz	*Chem. Rev.*	2000, **100**, 1604

1.3 Conjugated polymers vs. small molecules, absorption vs. emission

In most cases the fluorescent responses of PAEs and not colour change are discussed. Why? Changes in fluorescence are more

sensitive towards analytes than changes in absorption spectra, and fluorescence can be measured when the concentration of the sensor molecule is quite low. A typical concentration of PAE-sensors is in the range of 1-10 μM, based on the concentration of the repeat unit, while colorimetric sensors often work at much higher concentrations.

What makes conjugated polymers superior or complementary to small molecules and to nanoparticular sensors? In small molecules, a sensory appendage is attached to a single chromophore and therefore multivalency effects[7] are difficult to engineer in. In conjugated polymers one has one or several sensory appendages per repeat unit, and multiple point interactions are supported. This effect is particularly important for the sensing of large, biologically active molecules such as proteins, bacterial cells, or cell lysates. Conjugated polymer nanoparticles on the other side[8] are stable and show excellent optical properties but are significantly more difficult to functionalize than the linear PAEs.

1.4 Fluorescence in water: true blue

Most PAEs are highly fluorescent with ϕ up to unity, but only in dichloromethane, chloroform, or THF. The fluorescence quantum yield decreases in methanol or ethanol and drops again when water is the solvent, in which sensing often must be performed. The problem is exacerbated if yellow, orange or red emitting PAEs are made water soluble, while blue emitting PAEs such as **2-4**,[9] **6**,[10] **7**,[11] **8**,[12] and **9**[13] display relatively high fluorescent quantum yields in water (Figure 1). An interesting study was published by Schanze;[9] PAEs **3** and **4** show quantum yields of $\phi = 0.10$ and 0.19, while the red-emissive PAE **5** is almost non-fluorescent in water. Why are red and orange-emissive PAEs less fluorescent? As the energy difference between ground and excited states is lower than in the case of blue emitters, the excited state can easily couple to higher vibronic states of water. This is evidenced by the often observed increase in quantum yield when going from H_2O into D_2O.[14] According to the Einstein relation (band gap law[15]), the rate of the spontaneous emission factors in with ω^3 of the emission frequency, *i.e.* when going from an emission wavelength of 400 nm to one of 600 nm, the relative spontaneous emission rate drops and the emissive lifetime increases by a factor of roughly 3. As a consequence, the excited state has a longer time to interact with the environment and experiences dynamic quenching by the solvent and other internal conversion effects. Blue emissive PAEs show short fluorescence lifetimes, measured by multiple groups, ranging from 0.3 to 0.8 ns. Spontaneous blue emission is efficient (Figure 1). The short lifetime of the excited state does not allow for internal conversion and makes solvent less detrimental as external quenching agent. An interesting case study is the comparison of **2** to **9**; alkoxy **2** absorbs at 430 nm, while the formally alkyl-substituted PPE **9** absorbs at 374 nm. The authors assume that **9** does not aggregate, while **2** does aggregate in water. The proof for this claim is weak.
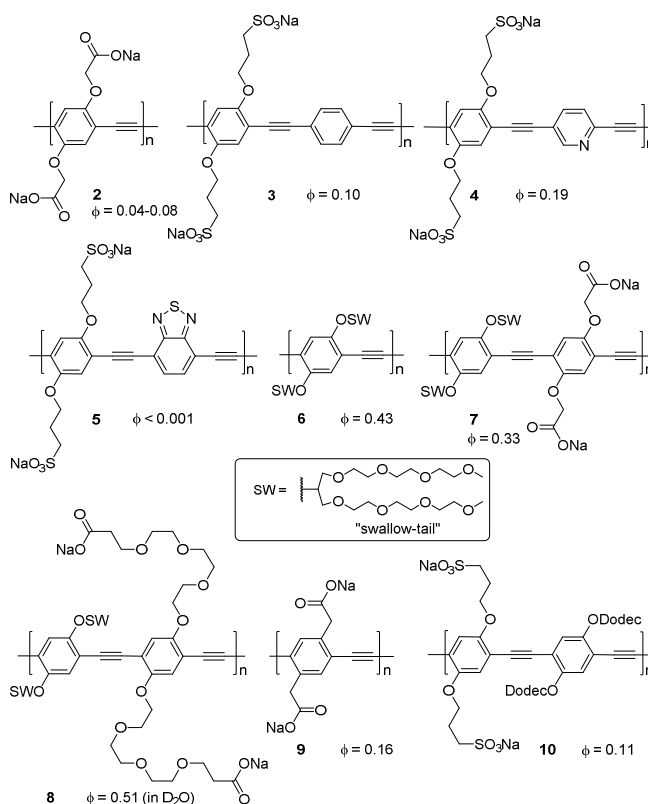

Figure 1. Quantum yield of different PAEs measured in water.

A simpler explanation would be, that the quantum yield is coupled to the emission wavelength, as the Einstein equation demands higher rates of spontaneous emission in fluorophores with blue-shifted emission. Shorter intrinsic emissive lifetimes then correlate with higher quantum yields, as the short-lived excited state is less affected by the environment.

1.5 Sensory responses of PAEs

PAEs and other conjugated polymers can transmit the binding to an analyte in different ways.

Quenching: Upon addition of an analyte, the fluorescence of the sensory polymer decreases. Static quenching and dynamic quenching are possible. In static quenching, the analyte forms a ground state complex with the sensor and after irradiation, the excited state is immediately and efficiently deactivated by the bound analyte. In dynamic quenching, the sensor molecule is excited and then, the excited molecule collides with a quencher and deactivates. Dynamic quenching is a diffusion-controlled process and can be excluded if the emissive lifetime of the polymer is < 1 ns. Dynamic quenching occurs if the fluorescence lifetime drops after the addition of a quencher. The most useful and simple tool for the mathematical evaluation of the quenching process is the Stern-Volmer

equation, which in the case of a static quenching process also gives the binding constant K_{SV}.

$$\frac{I_0}{I_{[Q]}} = 1 + K_{SV} \cdot [Q] \qquad \text{(eq. 1)}$$

In eq. 1 I_0 is the fluorescence intensity without added quencher Q, and $I_{[Q]}$ is the fluorescence intensity in the presence of the quencher Q at a specific concentration [Q]. K_{SV} is then the slope, the Stern-Volmer constant or the binding constant of the analyte to the sensor. There are some inherent assumptions that one should note. [Q] is the concentration of *free* quencher (difficult to determine), and *not* the total concentration of quencher (easy to determine). This is not a problem, as long the concentration of the sensor PAE (on a per repeat unit) is smaller than the inverse of the binding constant (then $[Q_{free}] \sim [Q_{total}]$); it means if one works at a 1 μM PAE solution, a K_{SV} up to 10^6 M^{-1} can be determined without any problem. The approximation that the total concentration of the quencher equals the free concentration of the quencher, holds then. Also, the assumption is that the quencher forms a 1:1 complex with the sensor molecule. At higher concentrations of PAEs the I_0/I plot becomes curved, as the concentration of the free quencher does not equal the (easily measured) total concentration of the quencher. The formation of a different quencher-PPE stoichiometry would also lead to curving.

If these assumptions do not hold, a more complex form of the Stern-Volmer equation has to be used (eq. 2), in which the fluorophore concentration $[F]_0$, the stoichiometry of the formed complex (n), and the easily measured total concentration of the quencher $[Q]_{tot}$ are considered.[16] I_0 is the fluorescence intensity of the PPE at a concentration $[F]_0$, without added quencher, $I_{[Q]}$ is the fluorescence intensity of the PPE in the presence of the quencher; α correlates the fluorescence intensities and concentrations of the two species; it is constant if the instrumental variables (*e.g.* slit width, excitation wavelength, sensitivity, *etc.*) and the identity of quencher and PAE are maintained. The solution to eq. 2 is obtained by a curve fitting analysis. Eq. 2 gives realistic values for K_{SV}.

$$I_{[Q]} = I_0 + \frac{\alpha}{2}\left[\left([F]_0 + n[Q]_{tot} + \frac{1}{K_{SV}}\right) \right. \\ \left. - \left\{\left([F]_0 + n[Q]_{tot} + \frac{1}{K_{SV}}\right)^2 - 4n[F]_0[Q]_{tot}\right\}^{0.5}\right] \qquad \text{(eq. 2)}$$

Superquenching: A related mechanism to quenching is superquenching. For example, one molecule of quencher seems to quench more than one polymer chain of the conjugated polymer under consideration. When very high quenching constants appear, one often assumes that many conjugated polymer chains form an excimer or a loose, emitting 3D aggregate. Then one quencher or binder molecule changes the optical properties of the whole ensemble.[17] These enhanced energy transfer aptitudes are common in conjugated polymer nanoparticles but also in electrostatic complexes.[16,18]

Ratiometric sensing is the change of the emission or absorption color of the sensor molecule upon the addition of an analyte. This color change can have different reasons. In simple PPEs, where the arenes do not contain hetero atoms, which ionic species can coordinate to, and in the absence of conjugating substituents, only the planarization of the backbone (under red shift of emission and absorption) will induce ratiometric changes.

If the PAEs under consideration either carries substituents that conjugate into the PAE system or heterocyclic building blocks that contain pyridine, quinoline or bipyridine units, direct colour changes by coordination to ionic species or by reaction with analytes in a dosimeter type fashion are observed.[19]

Turn on of fluorescence is possible through analyte-induced de-aggregation (see Figure 9) or through coordination of a metal cation to a covalently attached amino-functionality acting as internal quencher (Figure 15). Alternatively, turn on of fluorescence also occurs if (an)ionic PAEs are pre-reacted with (cat)ionic gold or other nanoparticles. These electrostatic complexes are non-fluorescent, but can be disrupted by the addition of a suitable analyte under restoration of fluorescence. Here, polyvalent interactions play a significant role, both in the formation as well as in the destruction of the electrostatic complexes by biological analytes, such as proteins, bacteria, cells and cell lysates. This is an induced fluorescence turn on, as the fluorescence of the PAE itself is artificially quenched and only restored upon addition of the (bio)analyte. The concept, however, is powerful and works well in water and has been exploited.[20]

1.6 The molecular wire effect

In 1995 Swager studied the quenching of the cyclophane-appended PPE **11** (M_n(GPC) = 6.5 x 10^4 g/mol) with paraquat (Figure 2). The molecular weight of the repeat unit of PPE **11** is 1106 amu, so the degree of polymerization P_n is approximately 60 repeat units, or around 120 phenyleneethynylene units featuring 60 binding appendages. The emission lifetime of **11** is τ = 0.64 ns. The values for P_n are probably a bit on the high end, as GPC tends to overestimate the molecular weight of rigid rod polymers.[21] The binding constant K_{SV} between **11** and paraquat (pq) was measured to 1.01 x 10^5 M^{-1} on a per repeat unit base. A similarly structured, monomeric cyclophane-attached dye showed a K_{SV} of 1.6 x 10^3 M^{-1}. As a consequence, on a per receptor basis, the PPE fares by a factor of 63 better (or is more sensitive) than the analogous small molecule dye. If higher molecular weight PPEs **11** are employed, the enhancement factor of 65 or so is not exceeded, it is the limit of enhancement.
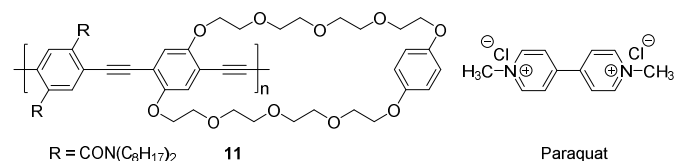

R = CON(C$_8$H$_{17}$)$_2$ **11**   Paraquat

Figure 2. Structure of cyclophane-appended PPE 11 and the employed analyte paraquat.

How to explain this enhancement of quenching? Upon coordination of one paraquat molecule the fluorescence of the 12-meric model PPE is completely quenched (Figure 3). If one takes 12 single, small molecule fluorophores and exposes them towards one molecule of paraquat, the emission intensity will – if we assume a static quenching mechanism– reduced by 1/12 th. Consequently, the enhancement factor is defined in this simple example by the number of receptors that are connected in a series. This concept is valuable as it imparts massive gains in sensitivity without appreciable cost.
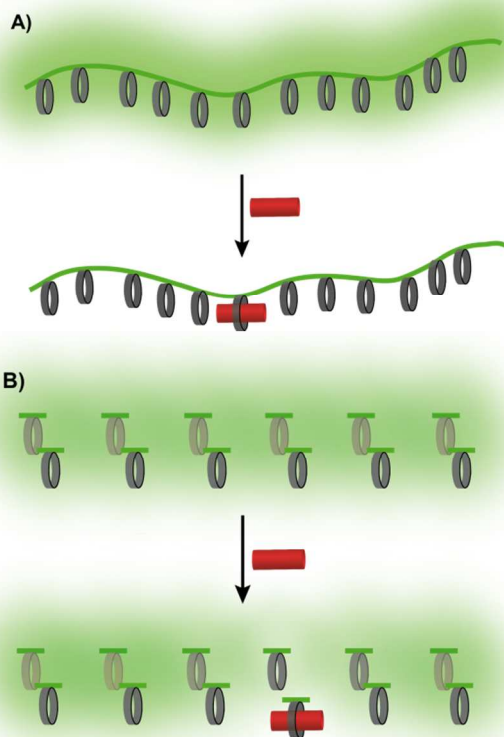
Figure 3. A) One paraquat molecule (red cylinder) quenches in this picture a PPE with 12 appended receptors; B) one paraquat molecule quenches one dye-appended receptor, the other ones are still fluorescent. In the shown picture the enhancement factor is 12.

In this picture, an exciton could be extended over 65 repeat units, which, for reasons that have to do with the size-dependent emissive wavelength dependence, is not realistic. Alternatively one exciton only extends over a small number of repeat units but moves along the chain and "services" 65 receptors, a more realistic picture. In how far quenching amplification by a factor of 65 is the upper limit in molecular wires is not clear. A series of carefully modified PPEs of consanguine structures and molecular weights would have to be prepared and tested. In the herein discussed example, the analyte was paraquat, a herbicide and poisonous to humans; a sensor for this material was of interest. As this was a proof of concept study, the synthesis of **11** and the proof of its sensitivity enhancement through the molecular wire effect was

seminal, even though this is not a field-compliant sensor technology.

1.7 Multivalency effects

If one analyte binds to more than one receptor (in a polymer chain), multivalent binding occurs, in which the binding constant with an analyte is higher than expected. An example is the quenching of the fluorescence of model compound **12** by lead ions in PIPES buffer (Figure 4). K_{SV} is measured to 600. When performing the experiment with polymer **2** under the same conditions, a K_{SV} of 8.8×10^5 is recorded. From experiments with paraquat for **12** and **2** we know that the molecular wire effect is around 58. After taking into account the molecular wire effect, **2** is by a factor of 26 more sensitive to Pb^{2+} ions than it should be. Acetate units from neighboring phenyleneethynylene repeat units contribute to the coordination of the lead ions (at low concentrations of **2**), and increase binding. The geometrical situation in **2-Pb^{2+}** is apparently not ideal, otherwise the effect would be considerably larger, as the second acetate group only leads to a 26-fold increase in binding and not to a 600-fold increase.
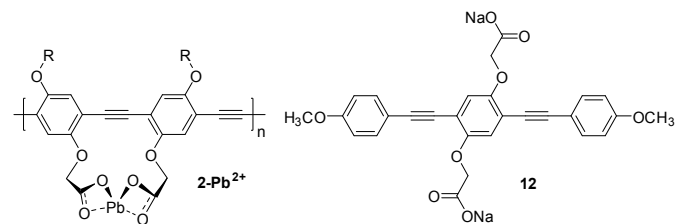

Figure 4. Pb-sensitive Polymer 2 and the corresponding model compound 12.

Also one could speculate that the monomer already shows "multivalency" as it has two acetate groups, but their geometrical arrangement, *para* to each other, on one benzene ring, apparently makes it difficult for them to bind to the same lead cation. Additional proof for the multivalency can be achieved at high concentration of **2**, as then lead salts precipitate **2** into a yellow non-fluorescent pellet. This type of polyvalency leads at higher concentrations to assaying through agglutination.

1.8 Compound sensors for PAEs

Compound or replacement sensors are systems in which a charged PAE such as **2** or **7** is connected to another charged species, particularly a cationic gold nanoparticle. The nanoparticle quenches the fluorescence of the PPEs as it forms a tight electrostatic complex in water. This complex disintegrates upon addition of an analyte that either binds to the nanoparticle or to the conjugated polymer. Turn on of the fluorescence results and it is dependent upon the structure of

the analyte. These sensors have been reviewed in depth recently and therefore are not discussed further here.[20]

2. Sensors using non-ionic PAEs

In this section we detail sensors that work with non-ionic PPEs, particularly as sensors for explosives. The prevailing mechanism for the detection of the explosives is fluorescence quenching. This concept works well, as most explosives are organic, electron poor nitro compounds; they form ground state complexes with the electron rich conjugated polymers and allow quenching the excited state of the polymer through excited state electron transfer into the low-lying LUMO of the explosive. As most conjugated polymers have short lifetimes (*vide supra*), their fluorescence is quenched by a static Stern-Volmer mechanism.

2.1 Sensing of nitroarenes, the detection of explosives

The sensor targets for pentiptycene-based PPEs **13** are buried land mines in war zones (Figure 5). These abandoned and buried land mines exude vapors of electron poor trinitrobenzene and dinitrobenzene, interacting strongly with **13**, quenching its fluorescence. **13** and relatives are obtained by a Sonogashira coupling of the diyne of pentiptycene with a suitable dialkoxy-diiodobenzene; **13** forms with an M_n of 1.4 x 10^5 g/mol and a PDI of 2.6. Swager and Yang propose that thin films of the polymers form porous morphologies. The absorption and emission spectra in solution and in the solid state (thin film) are almost identical, suggesting that there are no efficient interchain interactions (Figure 6).[22]
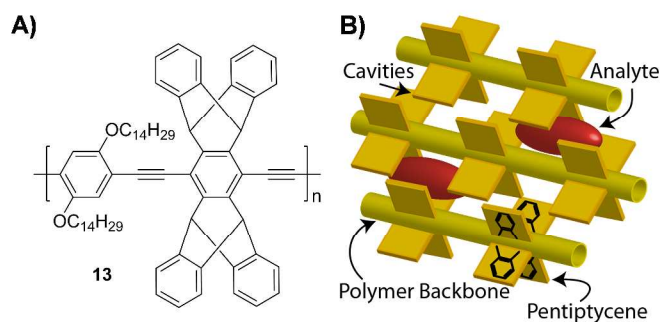

Figure 5. A) Structure of pentiptycene substituted PPE 13; B) fluorescence quenching mechanism of 13 through analytes, by occupying the cavities between the polymer rods set up by the pentiptycene groups.
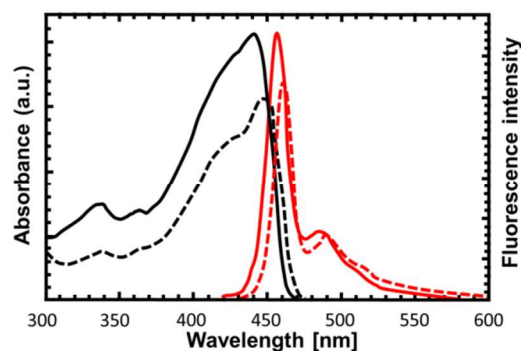

Figure 6. Absorption (black) and emission (red) spectra of 13 in solution (plain lines) and in solid state (dashed lines).

A series of nitroarenes was tested for their quenching ability of **13**. The analyte under consideration must show a first reduction potential that is > -1.6 V vs. SCE. The authors developed the following formula for the quenching efficiency FQ of **13**. The quenching efficiency FQ (eq. 3) is proportional to the binding constant of the quencher to the polymer (K_b), the vapour pressure (VP) and the term exp $(-\Delta G^0)^2$, connected to the reduction potential *via* the oxidation and reduction potentials of the polymer and the quencher respectively (eq. 4).

$$FQ \propto (VP)\exp[(-\Delta G^0)^2](K_b) \qquad \text{(eq. 3)}$$

$$\Delta G^0 = E(P/P^{+\cdot}) - \Delta E_{0-0} - E(Q/Q^{-\cdot}) \qquad \text{(eq. 4)}$$

Most dinitroarenes quench the fluorescence of **13** very well. Chloranil has both a high vapour pressure and a suitable reduction potential (0 V vs. SCE) but does not bind strongly to **13**, and therefore does not quench its fluorescence efficiently. While eq. 3 is useful, it still would have been important to determine the binding constants of **13** to nitroarens independently (in solution) and then look at the correlation. The binding constant K_b works here –in effect– as a scaling factor and allows adjusting any result by tweaking K_b to the desired value. Having said that, the introduction of iptycenes[23] and their application in explosives sensing was a major step in the field of fluorescent sensors, from a practical point of view, Swager has pushed this approach further and outlined the construction of a gadget for the detection of DNT and other nitrated explosive organic species.[24] A new development in this area was the use of thin lasing films.[25] However, in this case the polymer was a specifically substituted PPV.
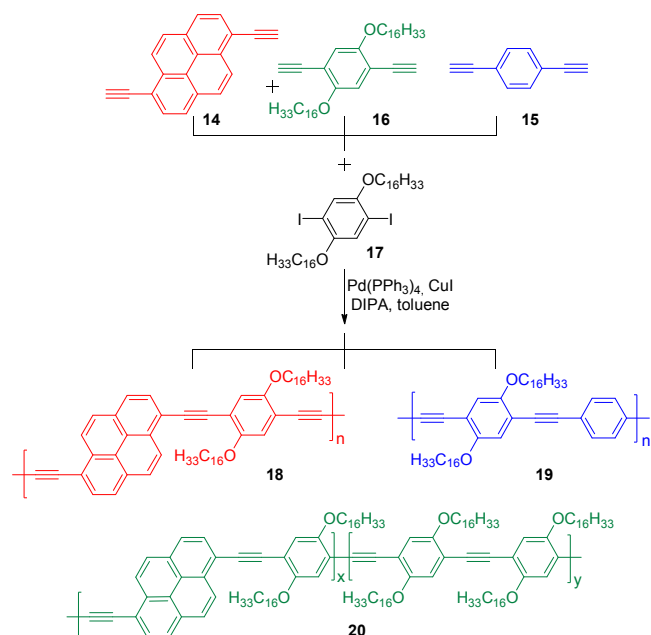
Scheme 1. Synthesis of pyrene-containing PAEs.

Other groups also looked at TNT sensing using PAEs. The group of Fang *et al.* prepared **18-20** (Scheme 1).[26] Thin films of the polymers **18** and **20** show quenching of their strong fluorescence when exposed towards aqueous solutions of TNT ($K_{SV} = 3.3 \times 10^4$ M^{-1}). The films –formed on glass slides– are around 20 nm thick with a spherical morphology ("ball-like", 300-500 nm sized features) according to AFM. This quenching is also observed in sea water, suggesting that the method might be useful in real life samples. **18** and **20** are by a factor of around 5 more sensitive towards TNT than the simple PPE **19**. The reason for the increased sensitivity is the better binding of the TNT to pyrene than to the benzene rings in PPE **19**. According to quantum chemical calculations, **18** and **20** are much more electron rich than **19**. There are several other noteworthy features in this work. The emissive lifetime was independent of the concentration of the quencher TNT, suggesting strongly that static quenching is operating. The exposure time is around 10 min until the measurements are made. Dinitrotoluene, a typical decomposition product of TNT, shows an apparent K_{SV} of 3.6×10^3, a factor of 10 lower than that of TNT, while nitrotoluene quenches the fluorescence of **20** with a K_{SV} of 1.3×10^3. The quenching is reversible and the films can be re-used after careful washing in ethanol. Overall this is an interesting concept, but it is not clear if the reported K_{SV} values truly represent binding constants, as the concentration of the fluorophore in the thin film is very high, and therefore the classic assumptions of the Stern-Volmer mechanism (K_{SV}/concentration of fluorophore) < 1 do probably not hold. Also, one would have to investigate superquenching effects in the thin films and see if actually pyrene excimers are formed. Towards that end, emissive lifetimes and also the absorption spectra and not only the excitation spectra of **18-20** should have been reported.
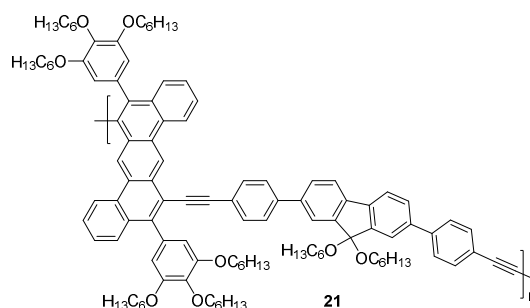

Figure 7. Structure of 21 to prepare electrospun materials.

The group of Pei *et al.* electrospun PAE **21** (Figure 7). A 4% solution of **21** with polystyrene and a porogen, sodium dodecyl sulphate, were processed. Long fibrils of approx. 500 nm in diameter resulted.[27] Thin films of **21** showed a red-shifted emission, as compared to the one obtained in solution, while the emission of the electrospun preparations is actually slightly blue-shifted as compared to that of **21** ($\lambda_{max,em.}$ = 427 nm, $\phi = 0.30$) in chloroform solution, suggesting that **21** is un-aggregated in the electrospun preparation. The authors determined the quenching of fluorescence by DNT in solution to give a static K_{SV} of 440 M^{-1}. Normal dialkoxy-PPEs show a K_{SV} of 30 M^{-1}. Consequently, **21** already interacts with DNT in solution. As electrospun film with porogen added, the fluorescence intensity decreases to 25% after exposure to DNT vapors after 1 h, while spin cast films of **21** do not show appreciable quenching. Use of the porogen increases the Brunauer-Emett-Teller (BET)-surface area of **21** from 11 to 42 m^{2}g^{-1}. The fluorescence is restored upon cleaning the sensor in an ammonia solution for 20 min. Seven cycles were reported with only small losses in the starting fluorescence intensity.

To increase the porosity of PAEs for explosives sensing, Dichtel and Novotney synthesized a microporous PPE **22** (Scheme 2)[28] coupling tribromobenzene to 2,5-diethynyl-1,4-dimethoxybenzene. Depending upon the reaction conditions, reaction solvent and the drying protocol, chemically identical samples of **22** with different fluorescence intensities and porosities were isolated. The best results with respect to fluorescence and porosity (S_{BET} = 259 m^{2}g^{-1}) were obtained for samples of **22** prepared in DMF and then washed with dioxane, followed by lyophilisation. **22** was exposed towards TNT in sand (a typical protocol that gives a 5 ppb equilibrium concentration of TNT in the atmosphere above the sand). In the best case the fluorescence of **22** was quenched to 40% of the starting value after 1 h. In films of **22** that were grown using toluene as solvent, fluorescence was almost unquenched even after 1 h of exposure. Overall, **22** is a powerful and interesting material to perform TNT sensing, even though the results of different species (*vide supra*) are difficult to compare, as there is no standardized protocol to assess sensing efficiency.
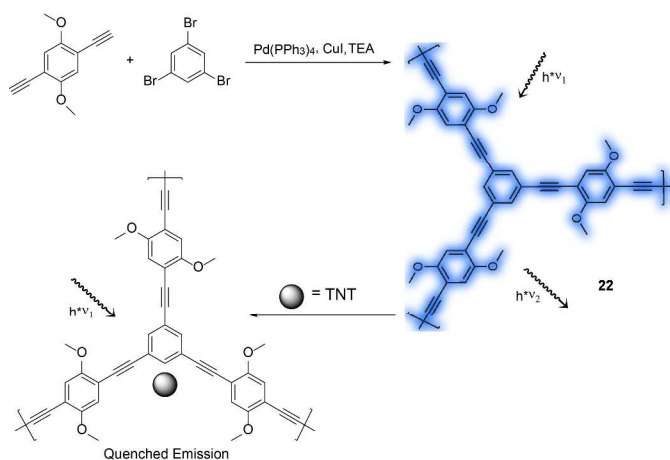
Scheme 2. Preparation of the PPE 22 and its behavior toward trinitrotoluene (TNT).

A similar approach uses silole-type PAEs.[29] Wang *et al.* prepared the polymers **25** and **26** (Scheme 3) and looked at their interaction with picric acid (PA) and TNT in solution. Both **25** and **26** are soluble in common solvents and show an M_n of around 19 and 15 kDa and PDIs of 1.02 and 2.3 for the polymers. **25** is formed as a hyperbranched PAE and not as a CMP[30] and therefore is quite soluble. The authors find, that K_{SV} in solution is 8.1 x 10^3 for **25** and 1.5 x 10^4 for **26** when quenched by picric acid and 0.8 x 10^3 and 1.1 x 10^3 for **25** and **26** towards TNT in solution. The linear polymer **26** is more sensitive towards TNT than the hyperbranched congener **25**, the authors rationalize that the increased steric bulk of **25** decreases the binding of the nitroarenes to the polymer. The binding model is shown in Figure 8.

2.2 Further uses of non-ionic PAEs in sensory applications

There are three sensor targets discussed in section 2.2. The detection of anions, detection of bio-relevant molecules (amines, sugars, *etc.*) and detection of metal salts using non-ionic PAEs. For the detection of anions, Kakuchi *et al.*[31] prepared butadiyne bridged **27** (M_n = 1.4 x 10^4, PDI = 2.6) by a Hay-type coupling of the corresponding monomer. In solution **27** self-assembles into a non-fluorescent aggregate in THF. Upon addition of fluoride as $Bu_4N^+F^-$, this aggregate breaks up and a fluorescent solution forms with a turn on factor > 10 and a significant red shift in emission (Figure 9). This turn on is explained by the break-up of the aggregates to give the fluorescence response of the single chains. This red-shifted turn on signal of **27** is not limited to fluoride, but also observed after the addition of benzoate and acetate. In the case of the addition of bromide and chloride to **27**, the fluorescence turn on is considerably weaker and the fluorescence is less red-shifted than in the case of fluoride. The probable reason for this behavior is the partial proton transfer from the urea to the anion, and therefore partial charge transfer to the polymer in direction to its anion, which shows a lower HOMO-LUMO

gap. While this is an interesting proof of concept experiment, it is not clear if such aggregates would form in water.
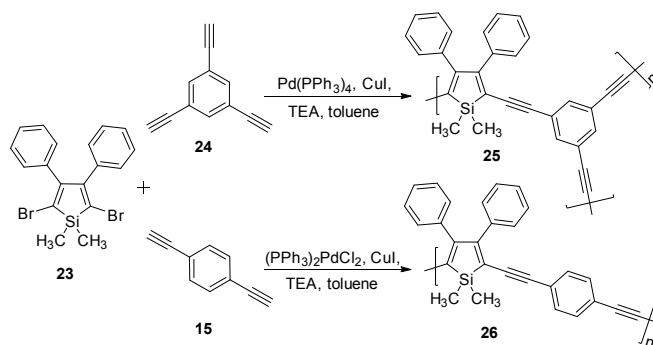
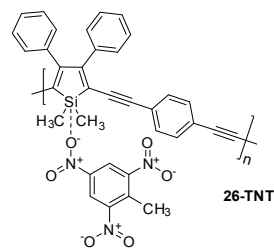**Scheme 3. Synthesis of 25 and 26 using Pd-catalyzed coupling.**

Figure 8. Interaction of polymer 26 with TNT.
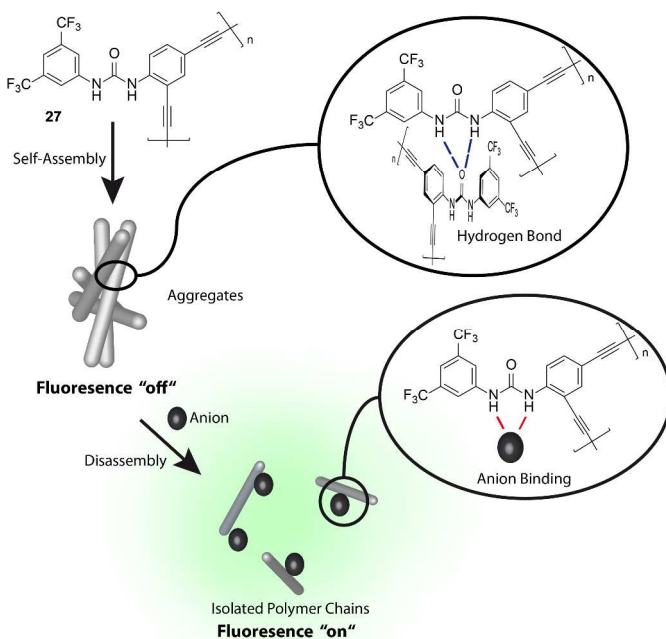

Figure 9. Structure of PPE 27 and mechanism of its anion-sensing action by de-aggregation through fluoride anions.

Fluoride anions[32] were detected using a novel combined approach where a blue emitting PPE-type oligomer in **28** and **30** is connected to a bis-TIPS-protected fluorescein-receptor (Figure 10), which at the same time is immobilized onto a glass surface to give **30**. In the absence of analyte, the glass surface emits blue. Upon exposure to fluoride the TIPS-groups are deprotected, forming **31** with free fluorescein, which then emits

green-yellow. Efficient energy transfer from the blue PE-oligomer to the fluorescein is observed.

Depending upon the ratio of the two fluorescence signals, one can quantitatively determine the amount of fluoride present, if a Stern-Volmer type equation is used, in which the ratio of fluorescence intensities $I_1(530 \text{ nm})/I_2(420 \text{ nm})$ are compared. The steeper the slope (2.4 for **28**, 0.4 for the fluorescein precursor **29**) upon exposure to fluoride is, the more sensitive the sensory system. Consequently, this approach gives a six-fold increase in sensitivity when comparing just the control **29** to the composite sensor **28**, where efficient Förster resonance energy transfer (FRET) is possible. This is an elegant and generally applicable concept for any type of sensor with a PAE-tail and a sensory head. The attachment of **30** or **31** to glass slides makes the system practical and useful.

Other uses for non-ionic PAEs were found by Hirose, Tobe *et al.* who prepared the PPE **32** (23 kDa, PDI 1.9) and the model compound **33** (Figure 11).[33] Both species react with aromatic amines, which quench their fluorescence, depending upon the chirality of the added amine. **33** binds to (*R*)-2-amino-1-propanol with a K_{SV} of 140. This number was corroborated using ^{1}H-NMR studies to give a K_b of 110. The selectivity of K_R/K_S for **32** is 3.6 by both NMR and K_{SV} titrations. In the case of the polymer **32** the K_{SV} is at low concentrations of (*R*)-2-amino-1-propanol 2.3×10^3, with a discrimination factor of 8, while, at higher concentrations of this amine, K_{SV} decreases to 1.1×10^3, but the selectivity K_R/K_S increases to 38. There are subtle effects that operate in **32**, making binding efficiency and chiral discrimination dependent upon the concentration of the analyte/quencher. Tobe et al. also studied chiral discrimination of valinol and 1-amino-2-propanol with **32**, but find that both binding and chiral discrimination are less pronounced for 2-amino-1-propanol.
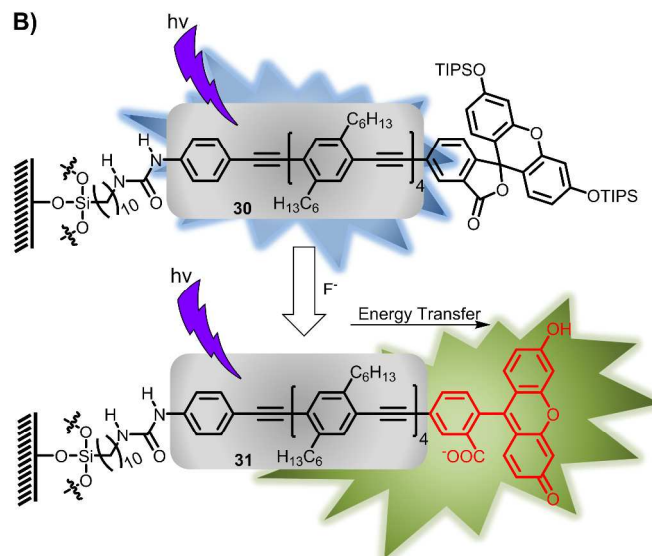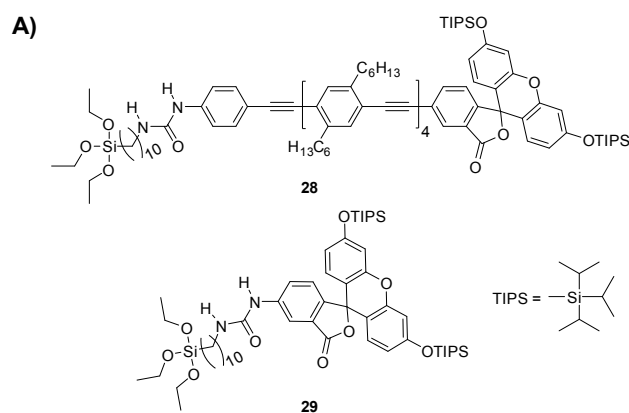

Figure 10. A) Structure of 28 and its model compound 29; B) general principle of the generation of ratiometric fluorescence response on exposure of 30 to fluoride anions to give 31.

34-36 and *rac* **35**/**36** were prepared (Figure 12).[34] **35** and **36** showed circular dichroism (CD)-effects[35] that were highly molecular weight and concentration dependent and inverted for high molecular weight fractions of **35** and **36**, due to the formation of "a different type of chiral higher-order structure". The high molecular weight fractions of **35** or **36** were fascinating as they form complexes with glycogen, pullulan and hyaluronic acids that are detected by the drastic changes in the CD spectra of the complexes, when compared to that of the polymers themselves. These experiments were conducted in water but needed around 4-5% of the sugar-analyte to be present.
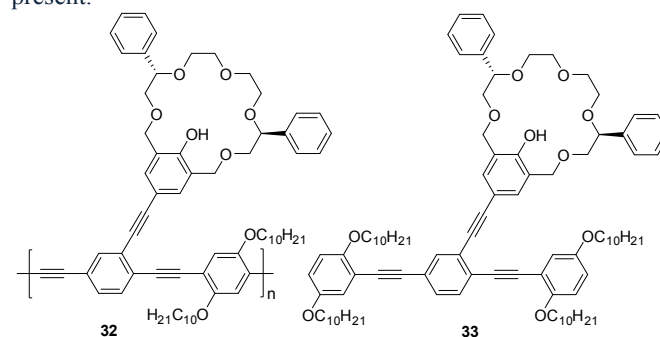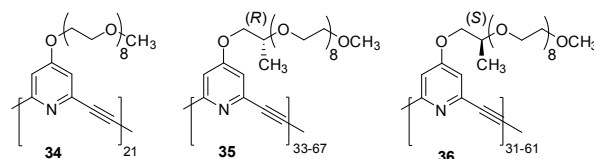

Figure 11. Structures of 32 and 33.

Figure 12. *Meta*-PPEs containing pyridine units for model sensor systems.

Inouye et al. have used **35** and **36** and their oligomers for further saccharide recognition, augmented by complexation

with copper ions.[36] While **35** and **36** are potentially important for advanced biosensing applications, their sensitivity is too low. A noteworthy feature is that one can modulate the CD-spectra of **35** or **36** by addition of metal ions, probably due to the formation of alternative supramolecular structures.

The sensing of metal cations[37] is observed with ionic PAEs, as they are well water soluble (*vide infra*), but some of the non-ionic PAEs are also metal detector systems, such as PAE **37** (Figure 13).[38,39] Exposure to Hg^{2+} salts in chloroform leads to a bathochromic shift of the absorption of **37** from 510 to 550 nm. The emission of **37** is quenched by Hg^{2+} salts with a K_{SV} of 2.5 x 10^5. Fan et al.[38] contend that the sensing action is due to the coordination of the mercury cations to the sulphur of the benzothiadiazoles, but is also an effect of mercury induced aggregation of the polymer chains. Chloroform is not a realistic solvent, as water would be preferred, but it is nevertheless an interesting proof of concept using **37**.
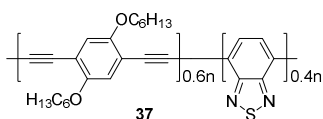

Figure 13. Structure of Hg^{2+}-sensitive benzothiadiazole substituted PAE 37.

The quest for Hg-sensitive PAEs was also tackled by Zaccheroni et al.[40] **39**, made from **38**, has an emission maximum at 540 nm, which suggests that it exists in an excimeric form in acetonitrile solution (Scheme 4). Addition of mercury salts to **39** leads to quenching; ppm-concentrations of Hg^{2+} are detected. It is surprising that the authors did not try to saponify **39** to be able to perform mercury sensing in aqueous solutions. **39** is nevertheless an attractive, amino acid substituted PPE, featuring sensory properties.
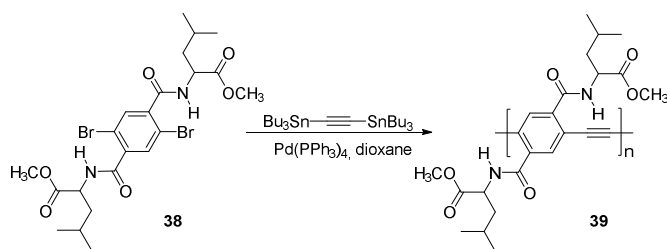
Scheme 4. Synthesis of Sterzo's amino acid PPE.

The group of Zhu prepared **40** and **41** and investigated their response to metal cations (Figure 14).[41] **40** was formed with an M_n of 3.2 kDa and a PDI of 1.9; suggesting a P_n of five repeat units with five receptors per polymer chain. The authors find that **40** is ultra-sensitive towards nickel cations in THF. At a concentration (per repeat) of 2 x 10^{-5} $molL^{-1}$, the addition of 1 x 10^{-7} $molL^{-1}$ Ni^{2+} quenches the fluorescence of **40** to 50%. Is that possible? If one assumes $P_n = 5$, then the concentration of whole polymer chains is 4 x 10^{-6} $molL^{-1}$, half of which, (2 x 10^{-6} $molL^{-1}$) *must* bind at least one Ni-cation to be quenched; one would need 10^{-6} $molL^{-1}$ Ni^{2+} to effect this quenching. Now, the reported sensitivity is a factor of 20 greater than expected. This

behaviour is currently unexplained. Interestingly, only open shell cations such as Co^{2+}, Mn^{2+} and Cu^{2+} show any appreciable quenching. Other metal cations such as Zn^{2+}, Cd^{2+}, and, surprisingly also Hg^{2+} do not show any response to metal cations. The formation of large aggregates that switch off their fluorescence in concert with the addition of Ni^{2+} might explain these results.
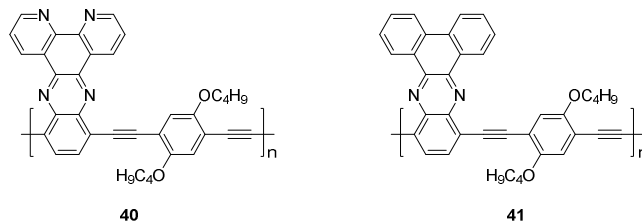

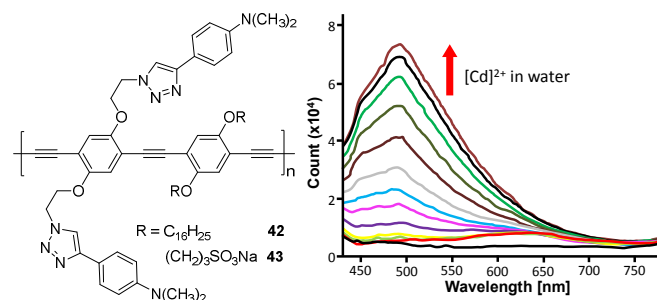**Figure 14. Metal-sensory PAEs with quinoxaline and phenanthroline units.**

Figure 15. Click-functionalized PAE 43 for the turn on-sensing of Cd^{2+}-ions in water.

An alternative way to detect binding of metal cations to conjugated polymers, under fluorescence turn on, is the click polymer **43** (Figure 15).[42] The presence of the dimethylamino group in **43** makes it non-fluorescent. Upon addition of Cd^{2+}-ions in water, fluorescence turn on was recorded, similar to the observations of Schweinfurth et al.[43] that demonstrated turn on fluorescence in simple click adducts. For **43** the experiment is performed in water, and while there are ionic auxiliary groups present, the binding action takes place at the triazole.

3. PAE sensors using ionic PAE

Ionic PAEs are powerfully water soluble materials. They are attractive as metal cation sensors but they are also capable to detect anions. Ionic PAEs are critical parts of compounded sensors, where electrostatic complexes with quenchers or adjuvants form, but they are also useful by themselves in bio-assays.

3.1 Ionic PAEs as metal sensors

Progress in the field of metal sensing with PAEs (until 2008) has been reviewed.[3] We will restrict ourselves towards ionic

PAEs as metal sensors that have appeared since 2009. The group of Wang *et al.*[44] prepared the two organometallic species, **44** and **45**, and investigated their metalloreactivity in water (Figure 16). The most dramatic effect was seen, if Ag$^+$ cations were added. The authors obtained binding constants of 1.5×10^5 M^{-1} according to both changes in absorption but also through analysis of the concentration dependent quenching data using the Stern-Volmer formalism.
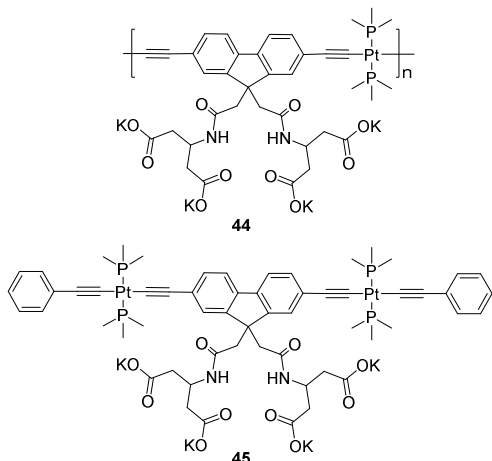

Figure 16. Pt-incorporated PAE 44 and the corresponding model compound 45.
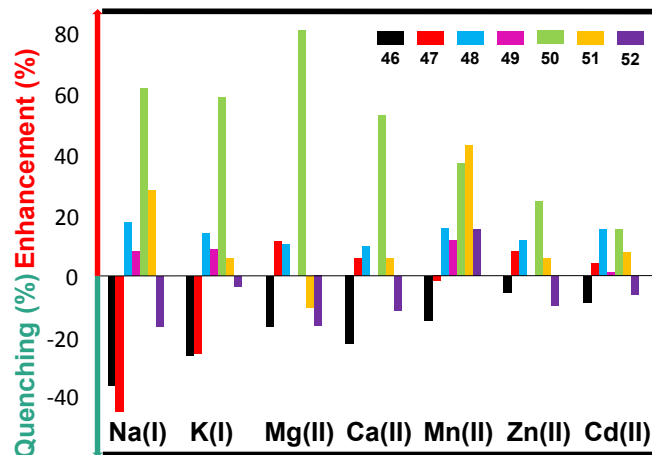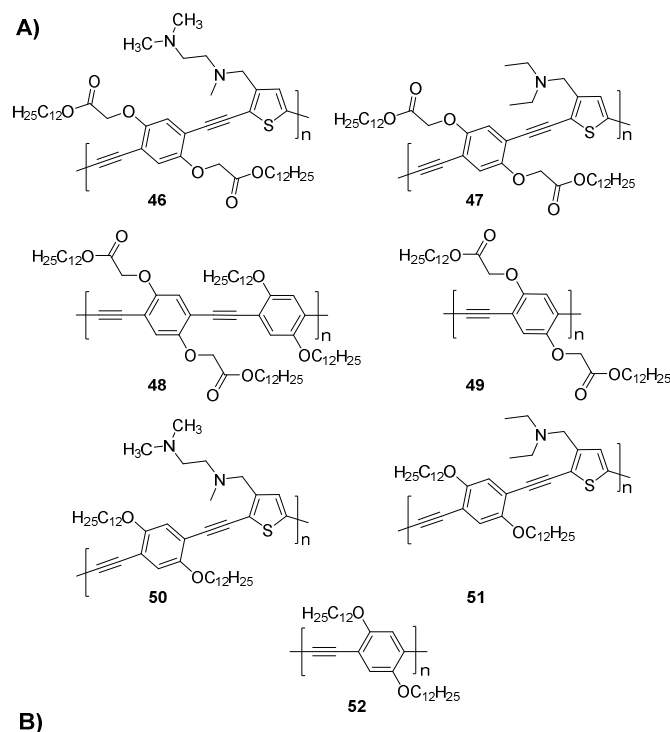

Figure 17. Molecules used in Fan's sensor array (A) to identify metal cations in THF (B).

Solutions of **44** turn visibly yellow upon addition of silver salts in water. None of the other tested metals (Hg^{2+}, Pb^{2+}, Cd^{2+}, *etc.*) elicited a strong response. The reason for the colour change of **44** is not clear, but there is no isosbestic point in the UV-spectra, even though **44** forms, according to the authors, a 1:1 complex with Ag$^+$ in water. The silver ions can also be detected by quenching of the phosphorescence (*vide supra*) of **44**. The introduction of the Pt-centres into the main chain of **44** changes the selectivity of this metal-organic PAE for binding of external metal cations, when compared to results that were obtained for polymer **2**.

An alternative metal sensory PAE **48**, was prepared (Figure 17).[45] **48** has both hydrophilic and ionic sulfonate groups but also dodecyloxy side chains. **48** shows its highest emissive quantum yields in water containing 30% THF. Sensing action is also best in this solvent mixture and the fluorescence intensity was reduced to about half, if the Fe^{3+} concentration was around 5 μM. In systems containing a different solvent composition, the quenching efficiency was lower. The relative maximum of fluorescence is explained by the presumed formation of aggregates. This is indirectly supported by the molecular weight determination of **48** using static light scattering, which gave (probably unrealistic for single chains) M$_w$ values of 9×10^6 Da. The authors contend that even in a good solvent like methanol the polymer chains are aggregated due to the amphiphilic character of **48**. While the authors collected the photophysical data, the emissive lifetimes were not reported.

In an extension of this concept, the same authors[46] prepared the polymers **46-52** and constructed a response pattern of this library for different metal cations (Figure 17). These PAEs were obtained with a P$_n$ of around 25-30 repeat units and show fluorescence quantum yields between $\phi = 0.06$ and $\phi = 0.25$ in THF-solution. Some of the polymers (**50** and **51**) increased fluorescence upon exposure to metal salts, while **46** and **47** showed some quenching. Overall, using this small array, a fingerprinting technique for the identification of metal cations was presented in this paper. The authors note, that the responses

are quite sensitive towards concentration of the different metal cations, which makes the use of this array challenging.

The group of Schanze investigated oligomers **53-58** (Figure 18).[47] **56** and **58** were Ca^{2+}-sensitive and show planarization induced red-shifts when 0.1 mmolL^{-1} of Ca^{2+} is added. In the cytoplasm of mammalian cells, the Ca^{2+} concentration is 0.2 µmolL^{-1}, as a consequence, these interesting oligomers are unfortunately not very useful as Ca^{2+}-binders in cell cultures. They were designed as proof of concept oligomers to test the effect of the degree of polymerization upon their photophysical properties. **54**, **56** and **58** show high K_{SV}-constants upon quenching with paraquat ($> 10^6$ M^{-1}). Higher metal binding efficiencies could probably be achieved, if different binding appendages were added to the oligomers and polymers.
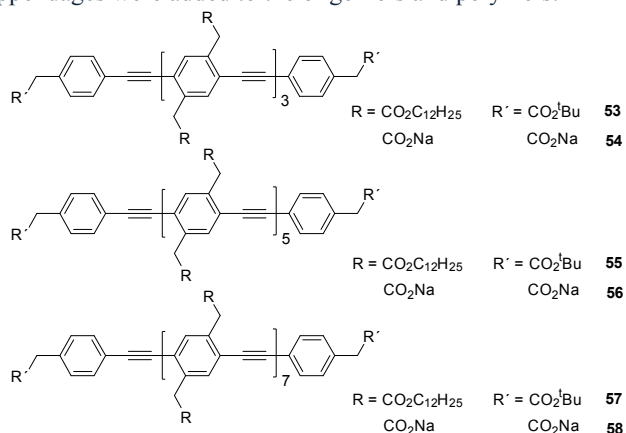

Figure 18. Oligomers synthesized by Schanze *et al*.

3.2 Structure-property relationships in PAE-based poly-electrolytes

Moon studied the interaction of PPE **59** with different acids; upon addition of tartaric acid, **59** forms dense aggregates, while acetic acid leads to loose ones. Tartaric acid has a pK_a = 2.98, while acetic acid (pK_a = 4.76) is a week acid.[48] The aggregation processes of **59** (Figure 19) are conveniently observed by optical spectroscopy. None of the higher molecular weight PPEs are soluble in water, but both acetic and tartaric acid render the shorter oligomers water soluble; for the tartaric acid based aggregates a red-shifted emission feature at around 500 nm is observed. This contribution should allow to tailor new PAEs and "titrate in" a desired aggregation state. This is even more attractive, if organic acids that have medical uses (aspirin *etc.*) are employed. If the aggregates then are released towards biological targets, such as cells *etc.*, the complexes might show biological activities.
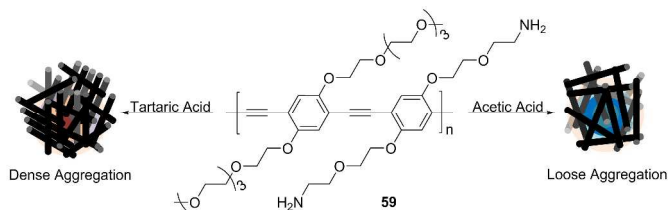

Figure 19. Schematic illustration of conjugated polymer nanoconstruct formation. The same batch of 59 produces different aggregation structures depending on the organic acid treatment.
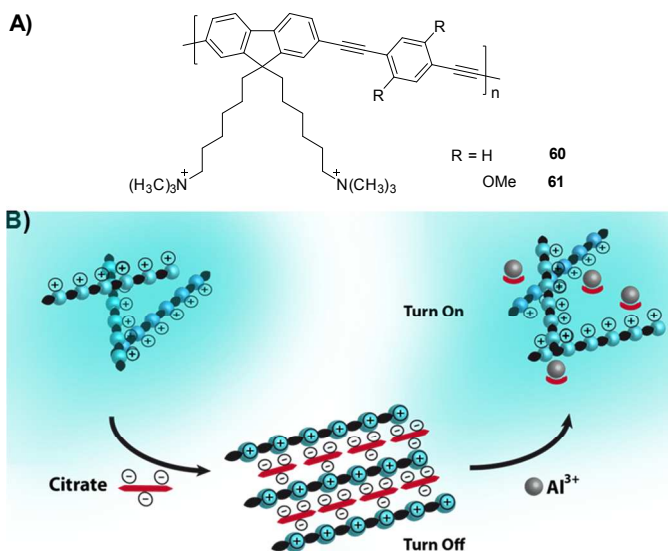

Figure 20. A) Molecular structure of Li's cationic PAEs 60 and 61; B) schematic illustration of the quenching menchanism trough induced aggregation by citrate and the turn on by Al^{3+}.

The group of Li *et al.* investigated the reaction of the two cationic PAEs **60** and **61** with citrate, resulting in efficient quenching of the PAEs' fluorescence through induced aggregation (Figure 20).[49] These aggregates were destroyed by the addition of aluminium cations to give an aluminium citrate complex plus the free, un-aggregated PAE, fluorescent again. The limit of detection (LOD) for Al^{3+} is around 0.4 µM. This LOD is reached with 10 µM solution of the PAE in the presence of 6 µM citrate solution. The sensor type was applied from pH 3 to pH 8. Other metal cations did not interfere as they apparently formed less strongly bound complexes with citrate. Other trivalent metal cations, such as Cr^{3+} or Ga^{3+} did not give any response. Consequently, this system is an excellent aluminium sensor.

Schanze *et al.* investigated a series of PAEs with branched carboxylates or branched ammonium side chains of the structures **62-67** (Figure 21).[50]
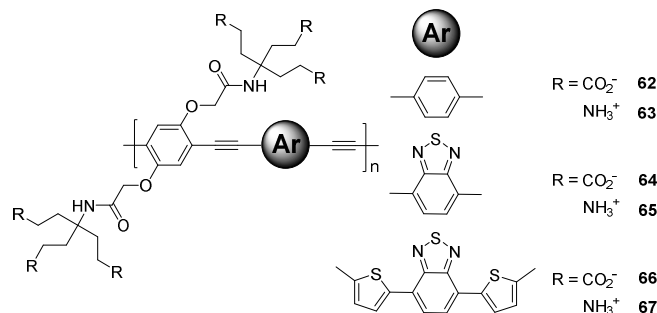
Figure 21. Structure of the branched PAEs 62-67.

In water (pH 9) the carboxylated PAE-copolymers **64** and **66** are still not very emissive, **64** has now a quantum yield ϕ in water of 0.7%, while **62** has a ϕ of 12% in water. Notable is that the ammonium-substituted polymer **63** has a similar ϕ of 13% in water as **62**. The authors contend that the bulky groups lead to twisting of the backbone and to a decrease of aggregation. Yet, the orange-red **64** and **65** are only weakly emissive.
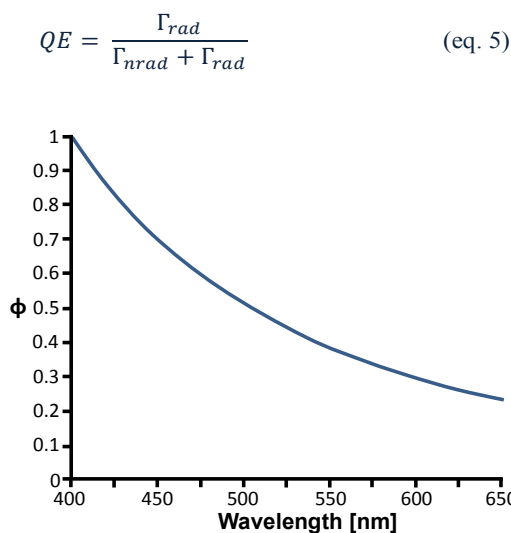
$$QE = \frac{\Gamma_{rad}}{\Gamma_{nrad} + \Gamma_{rad}} \qquad \text{(eq. 5)}$$

Figure 22. Quantum yield plotted over wavelength.

Why are **64** and **65** only weakly emissive? The catchall explanation for all of these issues is aggregation. However, aggregation is not the only effect here. If one looks at Einstein's law of spontaneous emission, then the emission efficiency and the inverse lifetime of the excited state is also (but not only) proportional to ω^3 (Figure 22). If the spontaneous emission rate for an emitter is arbitrarily set at 1.0 at 400 nm, at 650 nm the rate is reduced to around 0.23. This relation can only be held for similar chromophores and works only *via* the emission lifetimes. For a blue emitter such as dialkyl-PPEs, the fluorescence quantum yield is almost unity and the emission lifetimes range from 0.2-0.7 ns (short). As one can measure quantum yield and the total lifetime as the inverse of the total decay rate Γ_{rad}. For $\phi = 1$, the total decay rate equals the radiative decay rate $\Gamma_{tot} = \Gamma_{rad}$ and

$$\phi^{-1} = (\tau_{rad} + \tau_{nonrad})/\tau_{rad} \text{ and } \tau_{total} = (\tau_{rad} + \tau_{nonrad}) \text{ (eq. 6)}$$

Using this equation we can compute τ_{total} for **64** ($\tau_{total} = 24.3$ ns) and that of the PPE **62** ($\tau_{total} = 1.9$ ns), if one assumes a radiative life time (Table 3 in ref. 50, p. 4748) of $\tau_{rad} = 0.23$ ns and a quantum yield of $\phi = 0.13$. For **64** the values are $\tau_{rad} = 0.17$ ns and $\phi = 0.007$. Consequently, in **64** the excited state shows a total lifetime of $\tau_{tot} = 24.3$ ns, and therefore experiences massive radiationless decay. The effects are larger than expected, but in the case of **64** and **66**, coupling to higher vibrational states of water molecules need to be considered in addition to the charge transfer character of the polymer. Also, such acceptor-substituted polymers could experience external quenching by the solvent due to the position of their HOMO and LUMO.

From a practical point, it is not easy to make water soluble orange or red emitting polymers with high quantum yields and it is not clear how this problem will be overcome, even though the addition of more carboxylate groups helps with the quantum yield.

For successful biological sensors, the supply of yellow or orange emissive, water soluble polyelectrolytes is an important challenge, as biological systems and fluids fluoresce in the blue, an effect called "blue haze", background emission caused by aromatic amino acids, serum proteins, nucleobases and degradation products of porphyrine-type biomolecules.[51]

3.3 PPE and PAE biosensors

Water soluble PPEs and PAEs are attractive in biosensory applications. Zhang *et al.* prepared sophisticated star-shaped PPEs **72** and **73** by first making dendrimer **69**, carrying an iodobenzene head group, which is then copolymerized with the AB monomer **70** to give PPE **71** (Figure 23).[52] Quarterisation with bromoethane furnishes the cationic **72**. While the formed particles are 200 nm in diameter, they apparently do not aggregate and also show a two-fold enhanced fluorescence intensity in water when compared to the corresponding simple cationic PPE. According to the light scattering data, the simple cationic PPE shows aggregates sized 700 nm, suggesting that it is highly aggregated, contrary to **72**. Also **72** is much less cell toxic than the simple, non-nanoparticulate PPE-parents. The authors used **72** as cell-staining dye, where it performed superior to its simple counterpart and gave fluorescence co-localization with the mammalian cells. In **73** 50% of the amines were quarternized by a mix of bromoethane and a suitable brominated folic acid derivative. Both, **72** and **73** gave electrostatic complexes with short interfering RNA (siRNA).[53] These complexes were immune towards cleavage by RNAses, *i.e.* the electrostatic complexes stabilized the siRNA significantly. SiRNAs are proposed as possible anti-cancer therapeutics and as gene-silencing tools, but they are sensitive and do not invade cells easily; gene-delivery vehicles have to be deployed. **73**-siRNA complexes are ideal in transfecting HeLa-cells; the added folate increases the binding of the PPEs to the cells.[54] Transfection with the siRNA using **73** occurs

successful and gene silencing efficiency of almost 80% by this construct. These polyvalent carriers showed therefore massive gene knockdown and have great potential.
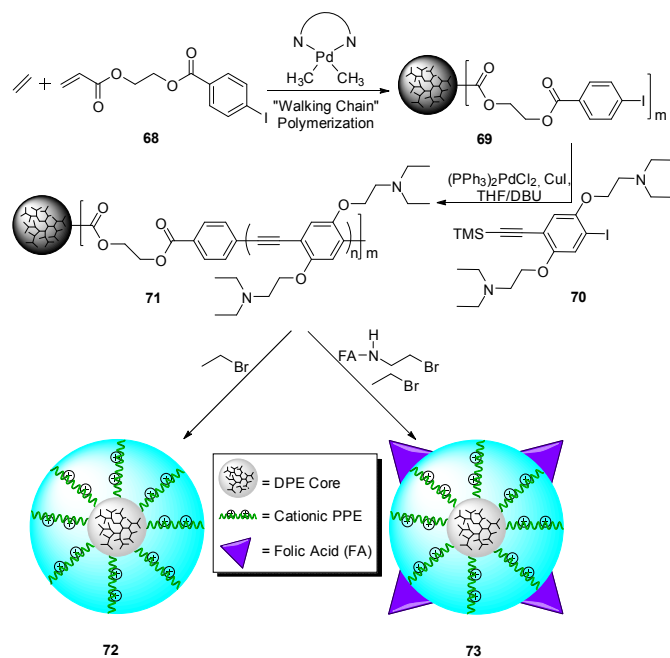

Figure 23. Synthesis of 72 and 73.

The detection of biological species, here G-quadruplex structures, were shown by the reaction of a complex of **4** with the quenchers **74-78** (Figure 24).[55] The quencher **75** did give the highest K_{SV} with **4** of up to 7×10^7 $M^{-1}s^{-1}$, while **74** quenches much less effective (2×10^7 $M^{-1}s^{-1}$). The complex of **76** and **4** has the highest stability but is also the one that detects human telomeres most reliably. The formation of a G-quadruplex-**76** complex releases the PPE, which reacts under fluorescence turn on.
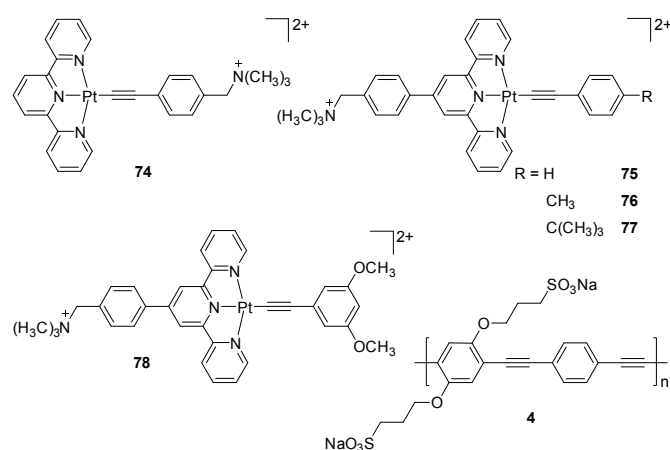

Figure 24. Pt-incorporated cationic spezies 4 and 74-78.

The PPE **4** was used for a quenching assay of catecholamines in water.[56] Horse radish peroxidase and H_2O_2 were non active in the presence of **4**, but upon addition of catecholamines, the fluorescence of the PPE was quenched through the formation of *ortho* quinones from the catecholamines. This method quantifies the presence of catecholamines and fared well in comparison to HPLC/MS. Depending upon the structure of the catecholamines, the detection limits varied from 10^{-6} to 10^{-7} $molL^{-1}$.
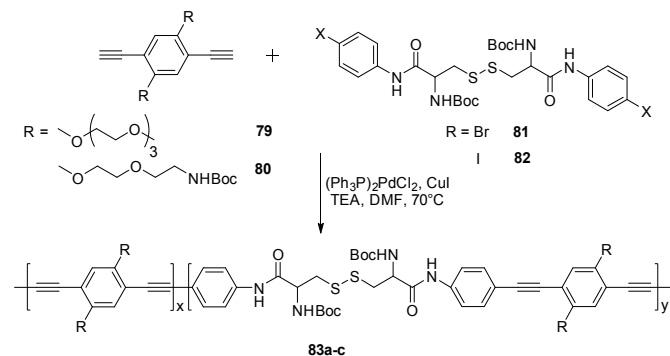
Scheme 5: Synthesis of cell staining PPEs.

The group of Moon *et al.* investigated **83a-c** as stains for HeLa cells. **83a-c** were produced by a clever mixed Sonogashira-Hay-type coupling that gives the desired copolymers in one shot (see Scheme 5 and

Table 2).[57] The introduction of the flexible monomers leads to different copolymers. When the ratio of **80** to **81** is unity, the authors obtain PAE **83c** after deprotection of the Boc-group, efficient in the staining of HeLa cells. The disulphide bridges allow **83c** to fold and make it therefore flexible and soluble. The polymers were endocytized into the Golgi apparatus as colocalization experiments show (
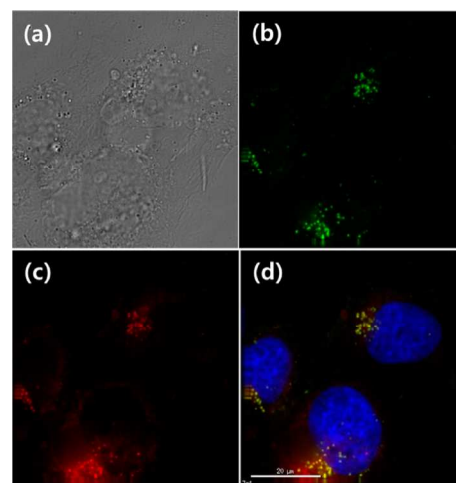
Figure 25).

Figure 25. Microscopic images of HeLa cells incubated with 83c. Accumulation of green fluorescent 82c (b) in the Golgi apparatus (c) is confirmed by overlapped signals (yellow) in the composed

image (d). (a) shows the corresponding contrast image. Reprinted with permission from (T. Vokata, J. H. Moon, *Macromolecules* 2013, *46*, 1253-1259). Copyright (2013) American Chemical Society.

Table 2. Physical properties of cell staining PPEs.

Polymer	Ratio	M_w [g/mol]	M_n [g/mol]	PDI	$\lambda_{max,abs}$ [nm]	$\lambda_{max,em}$ [nm]	ϕ [%]
83a	**79/81** 1:0	37400	16600	2.3	447	479	17
83b	**79/81** 1:1	97400	38400	2.5	453	478	32
83c	**80/81** 1:1	71100	32400	2.2	455	478	31

Conclusions

We have covered PAEs as sensory materials. The underlying principles that make PAEs useful were discussed and specific seminal examples were highlighted to introduce effects and the powerful concepts (superquenching, molecular wire, polyvalency, *etc.*) that are exploited in their sensor applications. Also, the underlying intrinsic physical properties of the PAEs were illuminated, demonstrating how they make PAEs useful. In the second part, specific applications of PAEs towards sensor targets were covered with the literature since 2009 under consideration. Here the later applications of ionic and non-ionic PAEs are highlighted.

Over all, PAEs are powerful polymers with freely adjustable structural, spectroscopic and binding properties. Their size puts them in the middle between small molecules and nanoparticles. Therefore, the advantages of both substance classes are unified in them. Variability in structure and size, stability and their attractive optical properties style PAEs into premier sensory molecules that can be tuned to observe almost any sensor target. The detection mechanisms for PAEs range from proton transfer to dosimetric reaction of an analyte with suitably substituted PAEs. PAEs are stable and easily prepared materials with a bright and captivating future.

Notes and references

[a] Organisch-Chemisches Institut, Ruprecht-Karls-Universität Heidelberg, Im Neuenheimer Feld 270, 69120 Heidelberg, FRG. [b]CAM, Centre of Advanced Materials, Im Neuenheimer Feld 225, 69120 Heidelberg, FRG.

[1] U. H. F Bunz, J. M. Imhof, R. K. Bly, C. G. Bangcuyo, L. Rozanski and D. A. V. Bout, *Macromolecules*, 2005, **38**, 5892; T. Miteva, L. Palmer, L. Kloppenburg, D. Neher and U. H. F. Bunz, *Macromolecules*, 2000, **33**, 652; U. H. F. Bunz, J. N. Wilson and C. G. Bangcuyo, *ACS Symp. Ser.*, 2005, **888**, 147; K. Seehafer, M. Bender and U. H. F. Bunz, *Macromolecules*, 2014, **47**, 922.

[2] M. I. Sluch, A. Godt, U. H. F. Bunz and M. A. Berg, *J. Am. Chem. Soc.*, 2001, **123**, 6447; J. Kim and T. M. Swager, *Nature*, 2001, **411**, 1030.

[3] U. H. F. Bunz, *Chem. Rev.*, 2000, **100**, 1604; U. H. F. Bunz, *Adv. Polym. Sci.*, 2005, **177**, 1; U. H. F. Bunz, *Macromol. Rapid Commun.*, 2009, **30**, 772.

[4] Q. Zhou and T. M. Swager, *J. Am. Chem. Soc.*, 1995, **117**, 12593.

[5] R. Chinchilla and C. Najera, *Chem. Rev.*, 2007, **107**, 874.

[6] S. Thorand and N. Krause, *J. Org. Chem.,* 1998, **63**, 8551.

[7] M. Mammen, S.-K. Choi and G. M. Whitesides, *Angew. Chem. Int. Ed.,* 1998, **37**, 2754.

[8] C. Wu, B. Bull, C. Szymanski, K. Christensen and J. McNeill, *ACS Nano,* 2008, **2**, 2415.

[9] X. Y. Zhao, M. R. Pinto, L. M. Hardison, J. Mwaura, J. Muller, H. Jiang, D. Witker, V. D. Kleiman, J. R. Reynolds and K. S. Schanze, *Macromolecules*, 2006, **39**, 6355.

[10] A. Khan, S. Müller and S. Hecht, *Chem. Commun.*, 2005, 584.

[11] R. L. Phillips, O. R. Miranda, C. C. You, V. M. Rotello and U. H. F. Bunz, *Angew. Chem. Int. Ed.*, 2008, **47**, 2590.

[12] K. Lee, H. J. Kim and J. Kim, *Adv. Funct. Mater.,* 2012, **22**, 1076.

[13] J. M. Koenen, X. Zhu, Z. Pan, F. Feng, J. Yang and K. S. Schanze, *ACS Macro Lett.*, 2014, **3**, 405.

[14] K. Klehs, C. Spahn, U. Endesfelder, S. F. Lee, A. Fürstenberg and M. Heilemann, *ChemPhysChem,* 2014, **15**, 637.

[15] L. M. Tolbert, S. M. Nesselroth, T. L. Netzel, N. Raya and M. Stapleton, *J. Phys. Chem.*, 1992, **96**, 4492.

[16] R. L. Phillips, O. R. Miranda, D. E. Mortenson, C. Subramani, V. M. Rotello and U. H. F Bunz, *Soft Matter*, 2009, **5**, 5042.

[17] H. A. Ho and M. Leclerc, *J. Am. Chem. Soc.,* 2004, **126**, 1384; H. A. Ho, A. Najari and M. Leclerc, *Acc. Chem. Res.* 2008, **41**, 168.

[18] I. B. Kim, M. H. Han, R. L. Phillips, B. Samanta, V. M. Rotello, Z. J. Zhang, and U. H. F. Bunz, *Chem. Eur. J.*, 2009, **15**, 449.

[19] C. G. Bangcuyo, M. E. Rampey-Vaughn, L. T. Quan, S. M. Angel, M. D. Smith and U. H. F. Bunz, *Macromolecules,* 2002, **35**, 1563.

[20] U. H. F. Bunz and V. M. Rotello, *Angew. Chem. Int. Ed.*, 2010, **49**, 3268.

[21] H. L. Ricks, U. H. Choudry, A. R. Marshall and U. H. F. Bunz, *Macromolecules*, 2003, **36**, 1424.

[22] J.-S. Yang and T. M. Swager, *J. Am. Chem. Soc.*, 1998, **120**, 11864.

[23] T. M. Swager, *Acc. Chem. Res.,* 2008, **41**, 1181.

[24] C. J. Cumming, C. Aker, M. Fisher, M. Fox, M. J. La Grone, D. Reust, M. G. Rockley, T. M. Swager, E. Towers and V. Williams, *IEEE Trans. Geosci. Remote Sens.,* 2001, **39**, 1119.

25 A. Rose, Z. Zhu, C. F. Madigan, T. M. Swager and V. Bulović, *Nature,* 2005, **434**, 876.

26 G. He, N. Yan, J. Yang, H. Wang, L. Ding; S. Yin and Y. Fang, *Macromolecules,* 2011, **44**, 4759.

27 Y. Y. Long; H. B. Chen, Y. Yang, H. M. Wang, Y. F. Yang, N. Li, K. A. Li, J. Pei and F. Liu, *Macromolecules,* 2009, **42**, 6501.

28 J. L. Novotney and W. R. Dichtel, *ACS Macro Lett*., 2013, **2**, 423.

29 W. Shu, C. Guan, W. Guo, C. Wang and Y. Shen, *J. Mater. Chem*., 2012, **22**, 3075.

30 U. H. F. Bunz, K. Seehafer, F. L. Geyer, M. Bender, I. Braun, E. Smarsly and J. Freudenberg, *Macromol. Rapid Commun*., **2014**, in press.

31 R. Sakai, A. Nagai, Y. Tago, S. Sato, Y. Nishimura, T. Arai, T. Satoh and T. Kakuchi, *Macromolecules,* 2012, **45**, 4122.

32 B. G. Imsick, J. R. Acharya and E. E. Nesterov, *Adv. Mater.,* 2013, **25**, 120; B. G. Imsick, J. R. Acharya and E. E. Nesterov, *Chem. Commun.,* 2013, **49**, 7043.

33 K. Hirose, S. Miura, Y. Senda and Y. Tobe, *Chem. Commun*., 2012, **48**, 6054.

34 H. Abe, K. Okada, H. Makida and M. Inouye, *Org. Biomol. Chem.,* 2012, **10**, 6930.

35 J. N. Wilson, W. Steffen, T. G. McKenzie, G. Lieser, M. Oda, D. Neher and U. H. F Bunz, *J. Am. Chem. Soc.,* 2002, **124**, 6830.

36 S. Takashima, H. Abe and M. Inouye, *Chem. Commun.,* 2012, **48**, 3330.

37 J. J. Bryant and U. H. F. Bunz, *Chem. Asian J.,* 2013, **8**, 1354.

38 S. J. Liu, C. Fang, Q. Zhao, Q. L. Fan and W. Huang, *Macromol. Rapid Commun*., 2008, **29**, 1212.

39 C. G. Bangcuyo, U. Evans, M. L. Myrick and U. H. F. Bunz, *Macromolecules,* 2001, **34**, 7592.

40 A. Ricci, M. Chiarini, M. T. Apicella, D. Compagnone, M. Del Carlo, C. LoSterzo, L. Prodi, S. Bonacchi, D. Villamaina and N. Zaccharoni, *Tetrahedron Lett.,* 2013, **54**, 303.

41 X. Liu, X. Zhou, X. Shu and J. Zhu, *Macromolecules,* 2009, **42**, 7634.

42 Y. Pourghaz, P. Dongare, D. W. Thompson and Y. Zhao, *Chem. Commun*., 2011, **47**, 11014.

43 D. Schweinfurth, K. I. Hardcastle and U. H. F. Bunz, *Chem. Commun.,* 2008, **44**, 2203.

44 C. Qin, W.-Y. Wong and L. Wang, *Macromolecules,* 2011, **44**, 483.

45 D. Shen, L. Wang, Z. Pan, S. Chemg, X. Zhu, and L.-J. Fan, *Macromolecules*, 2011, **44**, 1009.

46 H. Xu, W. Wu, Y. Chen and L.-J. Fan, *ACS Appl. Mater. Interfaces,* 2014, **6**, 5041.

47 F. Feng, J. Yang, D. Xie, T. D. McCarley and K. S. Schanze, *J. Phys. Chem. Lett*., 2013, **4**, 1410.

48 Y.-J. Ko, E. Mendez and J. H. Moon, *Macromolecules,* 2011, **44**, 5527.

49 H. Wang, F. He, R. Yan, X. Wang, X. Zhu and L. Li, *ACS Appl. Mater. Interfaces,* 2013, **5**, 8254.

50 S. H. Lee, S. Kömüdü, X. Zhao, H. Jiang, G. Moriena, V. D. Kleiman and K. S. Schanze, *Macromolecules,* 2011, **44**, 4742.

51 J. R. Lakowicz, Principles of Fluorescence Spectroscopy 3rd ed. Springer Heidelberg, 2006.

52 L. Zhang, Q.-H. Yin, J.-M. Li, H.-Y. Huang and B.-X Wang, *J. Mater. Chem*., 2013, **1**, 756.

53 L. Zhang, Q.-H. Yin, J.-M. Li, H.-Y. Huang, Q. Wu and Z.-W. Mao, *J. Mater. Chem*., 2013, **1**, 2245.

54 I.-B. Kim, H. Shin, A. J. Garcia, U. H. F. Bunz, *Bioconjugate Chem.,* 2007, **18**, 815.

55 C. Y.-S. Chung and V. W.-W. Yam, *Chem. Sci.,* 2013, **4**, 377.

56 H. Huang, Y. Gao, F. Shi, G. Wang, S. M. Shah and X. Su, *Analyst,* 2012, **137**, 1481.

57 T. Vokata and J. H. Moon, *Macromolecules,* 2013, **46**, 1253.